02

Changes in the optical functions of a $Bi_{0.6}Sb_{1.4}Te_3$ crystal when the plasmon and electronic transition

© N.P. Stepanov[1,2]

[1] Transbaikal State University,
672036 Chita, Russia
[2] Baikal State University,
664003 Irkutsk, Russia

e-mail: np-stepanov@mail.ru

Received May 27, 2023
Revised September 28, 2023
Accepted September 29, 2023

During the study of the reflection spectra of the $Bi_{0.6}Sb_{1.4}Te_3$ crystal, a deformation of the plasma edge was detected, which increases with a decrease in temperature. The analysis of the behavior of optical functions calculated from the reflection spectra using the Kramers–Kronig relations suggests that there is a convergence of the energies of the plasmon E_p and the electron transition between the nonequivalent extremes of the valence band ΔE, accompanied by an increase in the electron-plasmon interaction. The changes in the real and imaginary parts of the permittivity function, as well as the energy loss functions occurring during the convergence of E_p and ΔE are described. It is established that the convergence of E_p and ΔE leads to the splitting of the peak of the energy loss function into two maxima, the spectral position of which does not change with a decrease in temperature from 101 to 78 K.

Keywords: reflection spectra, optical functions, plasma oscillations, electronic transitions, electron-plasmon interaction.

DOI: 10.61011/EOS.2023.09.57343.5264-23

Introduction

The convergence of the plasma oscillations energy and the band gap energy in semiconductors and semimetals may have an effect on optical and photovoltaic characteristics of materials that are used to fabricate electronic and plasmonic components [1,2]. The authors of [3–7] have analyzed such convergence of plasmon energy E_p and band gap energy E_g theoretically. It was found that an instability of the electron system state may emerge when $\hbar\omega_p \approx E_g$, possibly resulting in an enhancement of plasma oscillations due to recombination of electron–hole pairs.

The convergence of energies E_g and $h\omega_p$ may be induced by doping, since it provides an opportunity to alter the density of free carriers (and, consequently, the energy of plasma oscillations) in a semiconductor within a wide range. However, the transition energies also change in this case due to the Burstein–Moss shift. In view of this, experimental studies into the electron–plasmon interaction are scarce and necessarily involve a targeted search for crystals with close energies of plasma oscillations and interband transitions.

The convergence of energies in electron and plasmon spectra may be achieved in Bi, $Bi_{1-x}Sb_x$ alloys, and a number of other narrow-gap semiconductors and semimetals (e.g., InSb, $Cd_{1-x}Hg_xTe$, PbTe, and $Pb_{1-x}Sn_xTe$ [8–14]). Crucially, narrow-gap semiconductors and semimetals differ from metals in that plasma oscillations in them have energy $\hbar\omega_p \approx kT$ and may be excited thermally. The same is also true of crystals of $Bi_2Te_3-Sb_2Te_3$ solid solutions, which have been studied extensively owing to their application in thermoelectric materials science. This is the reason why the electron–plasmon interaction may be observed in them. Intriguing features of temperature dependences of the magnetic susceptibility of $Bi_2Te_3-Sb_2Te_3$ crystals have indeed been discovered in [15]. It was found that these features are manifested upon convergence of plasmon energy E_p and energy ΔE of carrier transition between nonequivalent extrema of the valence band. Trends in variation of the indicated energies with temperature and the solid solution composition have been identified by analyzing the data on physical properties of $Bi_2Te_3-Sb_2Te_3$ crystals (see Fig. 1).

It can be seen from Fig. 1 that the $Bi_{0.6}Sb_{1.4}Te_3$ crystal, which has 70% of Sb_2Te_3 in the $Bi_2Te_3-Sb_2Te_3$ solid solution composition and exhibited a sharp reduction in diamagnetic susceptibility [15], is exactly the one where the convergence of energies of electron transitions and plasmons should be observed at low temperatures, offering valuable opportunities for examination of the electron–plasmon interaction. Thus, the aim of the present study was to examine experimentally the patterns of temperature variation of reflection spectra of a $Bi_{0.6}Sb_{1.4}Te_3$ crystal in the region where the effects of plasma behavior of free carriers are manifested.

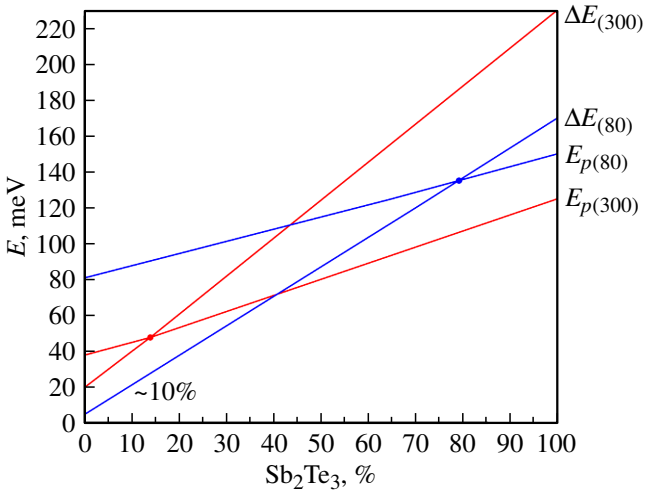

Figure 1. Dependences of plasmon energy E_p and energy ΔE of electron transition between nonequivalent extrema of the valence band at temperatures of 80 and 300 K on the percentage of Sb_2Te_3 in crystals of Bi_2Te_3-Sb_2Te_3 solid solutions [15].

1. Experimental procedure

The single crystal under examination was grown by the Czochralski method at the Baikov Institute of Metallurgy and Materials Science. The initial materials were Te, Sb, and Bi containing 99.9999 wt% of the base substance. The quality control procedure for crystals and the experimental technique were detailed in [16]. Reflectance spectra were recorded with an IFS-113V (Bruker) infrared Fourier spectrometer within the range from 370 to 2500 cm^{-1} with a resolution of 1 cm^{-1}. Measurements were performed with the use of unpolarized radiation in the $\mathbf{k} \parallel \mathbf{C}_3$, $\mathbf{E} \perp \mathbf{C}_3$ geometry, where $\mathbf{k}$ is the wave vector and $\mathbf{E}$ is the electric field vector of an electromagnetic wave. The angle of radiation incidence onto the vacuum–material interface deviated by no more than 8° from the normal to the mirror sample surface. Successive measurements of reflection spectra of the sample and the reference and their subsequent comparison were performed in order to determine reflectance R of the sample. The reference was an aluminum mirror with an absolute reflectance of 0.98 in the studied region.

The sample temperature was controlled by an evaporation cryostat that provided smooth temperature adjustment within the 78–300 K range and temperature stabilization with an accuracy no lower than 2 K.

2. Characterization and analysis of experimental results

The spectra of reflection of infrared radiation from the $Bi_{0.6}Sb_{1.4}Te_3$ crystal measured at temperatures of 78, 101, 173, 220, 250, and 292 K are presented in Fig. 2. Their shape is typical of plasma reflection, which is attributable to the resonance interaction between an electromagnetic wave and free carriers that oscillate longitudinally relative to the ion core with a certain intrinsic (plasma) frequency ω_p. In the case of multicomponent plasma, this frequency is written as

$$\omega_p^2 = \sum \frac{e^2 n}{\varepsilon_0 \varepsilon_\infty m^*}, \qquad (1)$$

where e is the electron charge, n and m^* are the density and the effective mass of free carriers, ε_0 is the dielectric constant, and ε_∞ is the high-frequency permittivity that characterizes the intensity of polarization processes in the high-frequency (relative to the plasma edge) spectral region. Summation is performed over all groups of free carriers shaping the polarization response.

It can be seen from Fig. 2 that the reflectance minimum shifts toward shorter wavelengths as the temperature decreases. This is indicative of an increase in plasma frequency and plasmon energy. The minimum reflectance

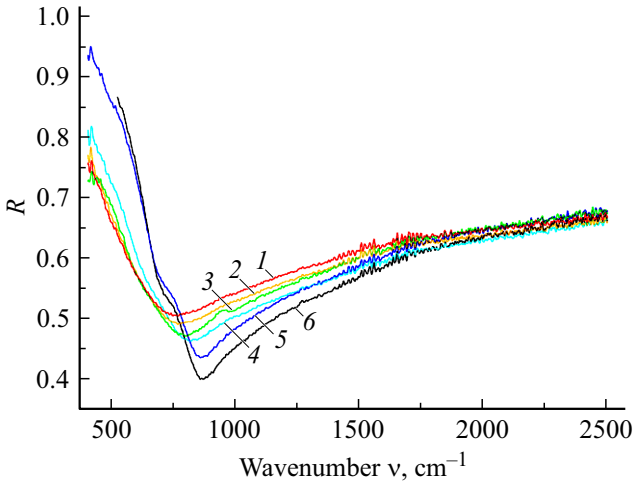

Figure 2. Reflectance R spectra of the $Bi_{0.6}Sb_{1.4}Te_3$ crystal measured at various temperatures: *1* — 292 K, *2* — 250 K, *3* — 220 K, *4* — 173 K, *5* — 101 K, *6* — 78 K.

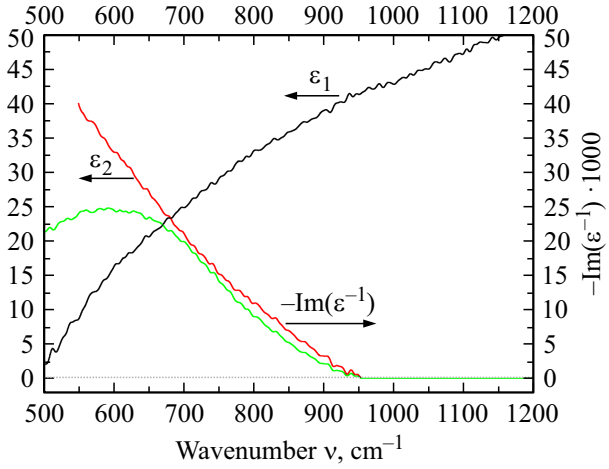

Figure 3. Spectra of ε_1, ε_2, and $-\mathrm{Im}\varepsilon^{-1}$ of the $Bi_{0.6}Sb_{1.4}Te_3$ crystal at a temperature of 292 K.

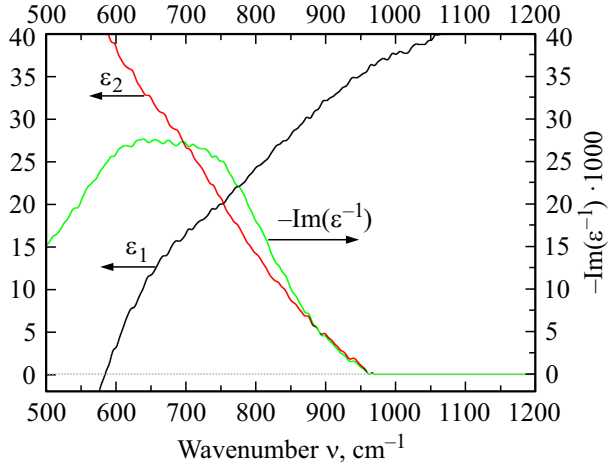

Figure 4. Spectra of ε_1, ε_2, and $-\mathrm{Im}\varepsilon^{-1}$ of the $Bi_{0.6}Sb_{1.4}Te_3$ crystal at a temperature of 173 K.

value decreases in the process, while reflectance R_∞ in the high-frequency region of the examined spectral range depends only weakly on temperature. It is also evident that the plasma edge gets deformed at temperatures below 200 K, and an inflection point emerges at 173 K. In the vicinity of this point, the reflectance decreases linearly as the frequency rises within the 620–760 cm^{-1} interval. This feature is not found in the reflection spectra recorded at 220, 250, and 292 K. When the temperature decreases further, the plasma edge deformation becomes more pronounced. As the temperature drops from 101 to 78 K, the minimum reflectance value decreases, and the spectral position of this minimum stabilizes.

Thus, the variation of reflectance spectra presented in Fig. 2 suggests that free-carrier plasma is affected by an additional process in the crystal, which intensifies as the temperature decreases. Its influence is already apparent in the reflection spectrum recorded at 220 K (curve *4* in Fig. 2) and is manifested in the form of a slight enhancement of reflectance at a frequency of 900 cm^{-1} (111 meV). Since these effects start to reveal themselves at a frequency of 760 cm^{-1} (94 meV) at 173 K (see above), the energy of the additional process decreases with increasing temperature at an approximate rate of 0.36 meV/K, while the plasmon energy, as was noted earlier, increases. This agrees with the data from Fig. 1, which suggests that an electron transition with energy ΔE may be the discussed additional process. This energy decreases with decreasing temperature due to shifting of the chemical potential level toward the heavy hole subband [16]. Crucially, the electron transition becomes „visible“ right in the vicinity of the plasma edge. This is attributable to the particular nature of plasma polarization response, which ensures that real part ε_1 of the permittivity function goes through zero near the plasma frequency [1]. This is the reason why the polarization influence of electron transitions, which is normally weak relative to the one of free carriers, is manifested in the spectra of optical functions (including the reflectance spectrum).

It follows from Fig. 1 that the rate of reduction of energy ΔE of the electron transition between nonequivalent extrema of the valence band in the $Bi_{0.6}Sb_{1.4}Te_3$ crystal is approximately equal to 0.23 meV/K, which is lower than the value of 0.36 meV/K obtained above. This is attributable, to a certain extent, to a faster shift of the chemical potential level within the 220–173 K interval. At low temperatures, the probability of electron transitions decreases, and the shift of the chemical potential level slows down accordingly.

It follows from the above that the plasmon energy and the electron transition energy converge in the $Bi_{0.6}Sb_{1.4}Te_3$ crystal as temperature decreases. An increase in the intensity of this transition translates into a reduction in the light hole density, which, according to (1), leads to a reduction in the plasmon energy. The diamagnetic susceptibility of the crystal also decreases [15]. The Hall coefficient in this crystal increases from 0.108 to 0.144 cm^3/K within the 78–350 K temperature range.

In order to analyze the obtained experimental data in more detail, real ε_1 and imaginary ε_2 parts of the permittivity function were calculated for all reflection spectra from Fig. 2 with the use of integral Kramers–Kronig relations between amplitude R and phase θ of a reflected wave:

$$\theta(\omega_0) = -\frac{2\omega_0}{\pi}\int_0^\infty \frac{\ln R^{-0.5}(\omega)d\omega}{\omega^2-\omega_0}. \qquad (2)$$

In most cases, $R(\omega)$ is determined experimentally, while $\theta(\omega)$ is calculated using expression (2). If $R(\omega)$ and $\theta(\omega)$ are known, one may reconstruct the frequency dependences of ε_1, ε_2, since the following relations are applicable at low angles of light incidence onto the material surface:

$$\varepsilon_1 = \frac{(1-R)-4R\sin^2\theta}{(1+R-2\sqrt{R}\cos\theta)^2},$$

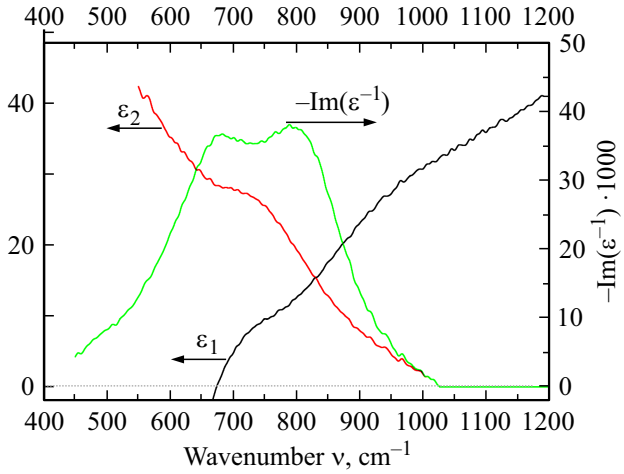

Figure 5. Spectra of ε_1, ε_2, and $-\mathrm{Im}\varepsilon^{-1}$ of the $Bi_{0.6}Sb_{1.4}Te_3$ crystal at a temperature of 101 K.

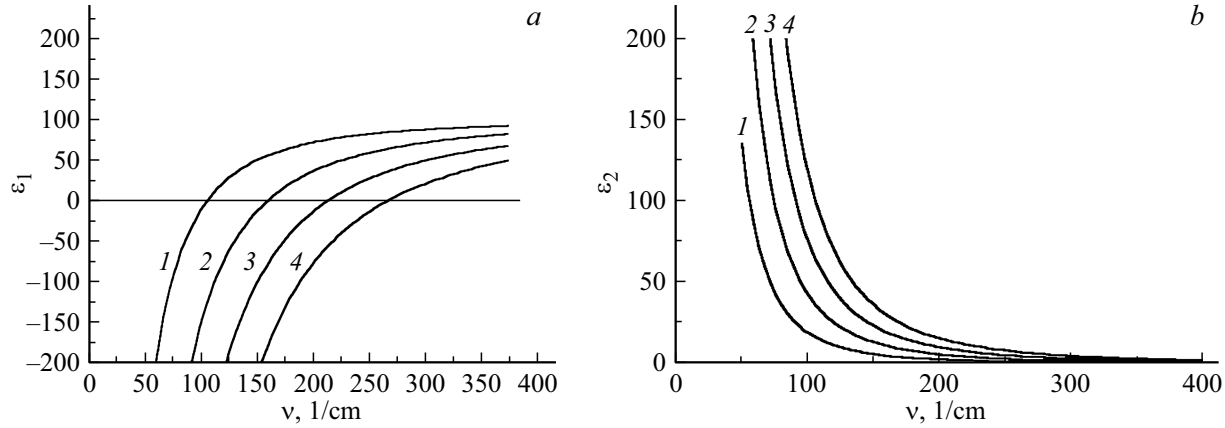

Figure 6. Calculation of the spectral dependence of real ε_1 (a) and imaginary ε_2 (b) parts of the permittivity function within the electron dispersion theory at different values of plasma frequency (ν_{pl}): *1* — 100, *2* — 150, *3* — 220 and *4* — 260 cm^{-1}.

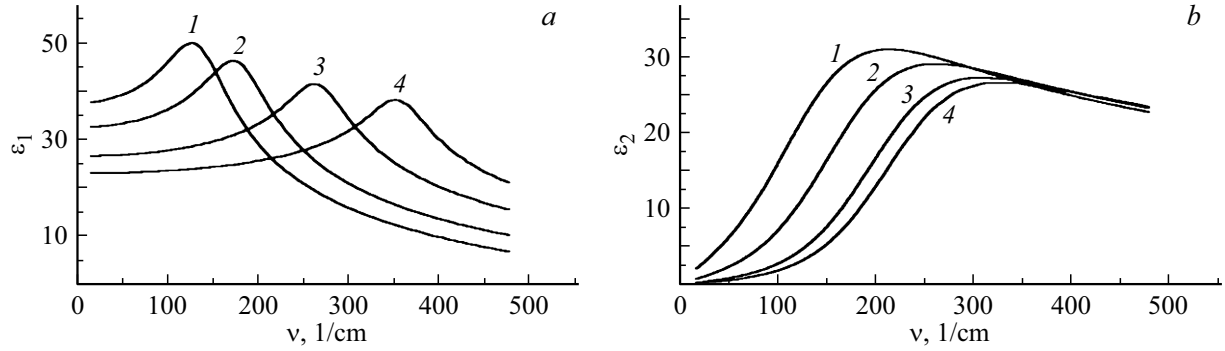

Figure 7. Calculation of the spectral dependence of real ε_1 (a) and imaginary ε_2 (b) parts of the permittivity function with interband transitions taken into account by the two-band model [14] at different values of interband transition energy (E_g): *1* — 140, *2* — 175, *3* — 260 and *4* — 350 cm^{-1}.

$$\varepsilon_2 = \frac{4(1-R)\sqrt{R}\sin\theta}{(1+R-2\sqrt{R}\cos\theta)^2}. \qquad (3)$$

The spectral dependences of ε_1, ε_2, and $-\mathrm{Im}\varepsilon^{-1}$ for the $Bi_{0.6}Sb_{1.4}Te_3$ crystal calculated at different temperatures with the use of relations (3) are presented in Figs. 3–5. Energy loss function $-\mathrm{Im}\varepsilon^{-1}$, which characterizes the frequency dependence of the dissipation intensity of the electromagnetic wave energy in a crystal, may be written as

$$-\mathrm{Im}\varepsilon^{-1} = \varepsilon_2(\varepsilon_1^2+\varepsilon_2^2)^{-1}. \qquad (4)$$

The data in Figs. 3–5 are grouped so that the relation between ε_1, ε_2, and $-\mathrm{Im}\varepsilon^{-1}$ at a fixed temperature is apparent in any individual figure and the variation of behavior of optical functions is easy to track when one analyzes a set of figures scaled in the same fashion. It can be seen from Figs. 3–5 that the frequency at which ε_1 goes through zero shifts toward higher frequencies as the temperature decreases. At the same time, the $\varepsilon_1(\upsilon)$ dependence deviates more and more significantly from the pattern typical of the response of free carriers in the classical electron dispersion theory (see the results of model calculation of this response in Figs. 6, a and 6, b).

Comparing, e.g., Figs. 5 and 6, b, one finds that the influence of the electron transition on the $\varepsilon_2(\upsilon)$ behavior also becomes more and more apparent. The nature of observed deviations is in agreement with the results of model calculations of the contribution of interband transitions to the real and imaginary parts of permittivity within the two-band model [17] (see Figs. 7, a and 7, b). This verifies the assumption that the shape of spectral dependences of ε_1 and ε, which are shown in Figs. 3–5, is affected by the electron transition.

Its influence is also noticeable in the behavior of $-\mathrm{Im}\varepsilon^{-1}(\upsilon)$ temperature dependences, which provide a clear illustration of the impact of convergence of the plasmon energy and the electron transition energy. It follows from the comparison of Figs. 3–5 that the peak of the energy loss function splits into two maxima under the influence of the electron–plasmon interaction that intensifies at lower temperatures. This may be attributed to the direct influence of the electron transition: its contribution to polarization and absorption processes becomes comparable in magnitude to the response of free carriers around the frequency at which ε_1 goes through zero. In addition, the results of theoretical analysis of the impact of convergence

of the plasmon energy and the electron transition energy (see above) suggest that plasma oscillations should intensify in this case due to recombination of electron–hole pairs with the emission of plasmons. The increase in absolute values of the energy loss function and the area under the $-\mathrm{Im}\varepsilon^{-1}(\nu)$ curve, which is seen in Figs. 4 and 5 at lower temperatures, indicates that this process also occurs in the studied $Bi_{0.6}Sb_{1.4}Te_3$ crystal.

Conclusion

We note in conclusion that the convergence of the plasmon energy and the energy sufficient for electron transitions from the heavy hole subband to the light hole one may facilitate the formation of a distinct state of the electron system. Specifically, it was demonstrated theoretically in [14] that two stable states of the electron system may form under induced plasma resonance in a semiconductor in an alternating electric field if the plasmon energy is sufficient for impact ionization. In accordance with (1), an increase in the density of free carriers then leads to an increase in the plasma frequency and, consequently, the transition to off-resonance conditions and termination of impact ionization. At the same time, the process of recombination of inequilibrium carriers, which reduces the plasma frequency and the plasmon energy, facilitates the convergence of E_p and ΔE and the activation of carriers by plasmons. Therefore, the stabilization of the plasma minimum position, which does not shift in frequency as the temperature goes down from 101 to 78 K (see Fig. 2), and the emergence of two well-defined maxima in the spectral dependence of the energy loss function (see Fig. 5) may also be related to the process that was characterized theoretically in [7].

Funding

This study was supported financially by the Government of Zabaykalsky Krai and grant No. 22-22-20055 from the Russian Science Foundation (https://rscf.ru/project/22-22-20055/).

Conflict of interest

The authors declare that they have no conflict of interest.

References

[1] V.V. Klimov. *Nanoplazmonika* (Fizmatlit, M., 2009) (in Russian).
[2] E.A. Pashitskii, V.I. Pentegov. Low Temp. Phys., **34**, 113 (2008).
[3] P.A. Wolff. Phys. Rev. Lett., **24**, 266 (1970).
[4] N.S. Baryshev. Fiz. Tekh. Poluprovodn., **9**, 2023 (1975) (in Russian).
[5] P.M. Platzman, P.A. Wolff. *Waves and Interactions in Solid State Plasmas* (Academic, 1973).
[6] A. Elci. Phys. Rev. (b), **16**, 5443 (1977).
[7] P.N. Shiktorov. Fiz. Tekh. Poluprovodn., **20**, 1089 (1986) (in Russian).
[8] E. Gerlah, P. Grosse, M. Rautenberg, M. Senske. Phys. Stat. Sol. (b), **75**, 553 (1976).
[9] J.G. Broerman. Phys. Rev. (b), **2**, 1818 (1970).
[10] M. Grynberg, R. Le Toulles, M. Balkanski. Phys. Rev. (b), **9**, 517 (1974).
[11] J.G. Broerman. Phys. Rev. (b), **5**, 397 (1972).
[12] A. Nanabe, D. Noguchi, A. Mitsuishi. Phys. Stat. Sol. (b), **90**, 157 (1978).
[13] P. Tussing, W. Rosental, A. Hang. Phys. Stat. Sol. (b), **52**, 451 (1972).
[14] P. Alstrom, H. Nielsen. J. Phys. C: Solid State Phys., **14**, 1153 (1981).
[15] N.P. Stepanov, M.S. Ivanov. Semiconductors, **56**, 879 (2022).
[16] N.P. Stepanov, A.A. Kalashnikov, O.N. Uryupin. Semiconductors, **55**, 637 (2021).

Translated by D.Safin